Mimicking the Membrane-Mediated Conformation of Dynorphin A-(1–13)-Peptide: Circular Dichroism and Nuclear Magnetic Resonance Studies in Methanolic Solution†

C. Roy D. Lancaster,‡,§ Prasanna K. Mishra,∥ Donald W. Hughes,⊥ Serge A. St.-Pierre,#,○ Aksel A. Bothner-By,∥ and Richard M. Epand*,‡,⊥

Department of Biochemistry, McMaster University, Health Sciences Centre, 1200 Main Street West, Hamilton, Ontario, Canada L8N 3Z5, Department of Chemistry, McMaster University, Hamilton, Ontario, Canada L8S 4M1, NMR Facility for Biomedical Studies, Department of Chemistry, Carnegie-Mellon University, Mellon Institute, 4400 Fifth Avenue, Pittsburgh, Pennsylvania 15213, and Department of Physiology and Pharmacology, Faculty of Medicine, University Hospital Centre, Sherbrooke, Québec, Canada J1H 5N4

Received November 27, 1990; Revised Manuscript Received February 15, 1991

ABSTRACT: The structural requirements for the binding of dynorphin to the κ-opioid receptor are of profound clinical interest in the search for a powerful nonaddictive analgesic. These requirements are thought to be met by the membrane-mediated conformation of the opioid peptide dynorphin A-(1–13)-peptide, Tyr[1]-Gly[2]-Gly[3]-Phe[4]-Leu[5]-Arg[6]-Arg[7]-Ile[8]-Arg[9]-Pro[10]-Lys[11]-Leu[12]-Lys[13]. Schwyzer has proposed an essentially α-helical membrane-mediated conformation of the 13 amino acid peptide [Schwyzer, R. (1986) *Biochemistry 25*, 4281–4286]. In the present study, circular dichroism (CD) studies on dynorphin A-(1–13)-peptide bound to an anionic phospholipid signified negligible helical content of the peptide. CD studies also demonstrated that the aqueous–membraneous interphase may be mimicked by methanol. The 500- and 620-MHz ^{1}H nuclear magnetic resonance (NMR) spectra of dynorphin A-(1–13)-peptide in methanolic solution were sequence-specifically assigned with the aid of correlated spectroscopy (COSY), double-quantum filtered phase-sensitive COSY (DQF-COSY), relayed COSY (RELAY), and nuclear Overhauser enhancement spectroscopy (NOESY). 2-D CAMELSPIN/ROESY experiments indicated that at least the part of the molecule from Arg[7] to Arg[9] was in an extended or β-strand conformation, which agreed with deuterium-exchange and temperature-dependence studies of the amide protons and analysis of the vicinal spin–spin coupling constants $^3J_{HN\alpha}$. The results clearly demonstrated the absence of extensive α-helix formation. χ_1 rotamer analysis of the $^3J_{\alpha\beta}$ demonstrated no preferred side-chain conformations.

Dynorphin A is an extraordinarily potent opioid peptide first isolated from the porcine pituitary (Goldstein et al., 1979). Since then it has been purified from the rat pituitary (Goldstein et al., 1981) and the porcine duodenum (Tachibana et al., 1982) and has been identified in the mammalian spinal chord and dorsal root ganglia (Botticelli et al., 1981), in the bovine adrenal medulla (Lemaire et al., 1982), and in the placenta (Lemaire et al., 1983). A considerable specificity of dynorphin for the κ-opioid receptor (Chavkin & Goldstein, 1981; Chavkin et al., 1982) has been reported. The different specificities of the enkephalins (δ), β-endorphin (ε), and dynorphin (κ) for the different receptor types is particularly striking, because they all possess the same N-terminal tetrapeptide sequence (Morley, 1983). κ-Agonists are of profound clinical interest because κ-opioid receptors have been shown to mediate analgesia with low addictive potential (Millan, 1990). The N-terminal fragment dynorphin, A-(1–13) (Tyr[1]-Gly[2]-Gly[3]-Phe[4]-Leu[5]-Arg[6]-Arg[7]-Ile[8]-Arg[9]-Pro[10]-Lys[11]-Leu[12]-Lys[13]), has approximately the same high potency (Goldstein et al., 1979; Tachibana et al., 1982) and κ-selectivity (Chavkin & Goldstein, 1981; Chavkin et al., 1982) as the natural 17 amino acid peptide so that most of the attention has focused on the 13 amino acid peptide.

The molecular basis of dynorphin's unusual ability to bind with high affinity to multiple opioid receptors is not known, but it may involve interaction with lipids. Sargent and Schwyzer (1986) have emphasized the importance of the membrane lipid phase as a catalyst for peptide–receptor interactions. The flexible peptide agonist is assumed to have little, if any, order in the intercellular fluid. This assumption is compatible with CD[1] (Maroun & Mattice, 1981; Kojro et

† This work was supported by a grant from the Natural Sciences and Engineering Research Council of Canada. This work represents part of a thesis submitted by one of the authors (C.R.D.L.) to the School of Graduate Studies at McMaster University in partial fulfillment of the requirements for the degree Master of Science.

‡ Department of Biochemistry, McMaster University.

§ Present address: Max-Planck-Institut für Biophysik, Abteilung Molekulare Membranbiologie, Heinrich-Hoffmann-Str. 7, D-W-6000 Frankfurt/Main 71, Germany.

∥ NMR Facility for Biomedical Studies, Department of Chemistry, Carnegie-Mellon University.

⊥ Department of Chemistry, McMaster University.

Department of Physiology and Pharmacology, Faculty of Medicine, University Hospital Centre, Sherbrooke.

○ Present address: INRS-Santé, Pavillon Gamelin, 7401 Hochelaga, Montréal, Québec H1R 1G6.

[1] Abbreviations: CAMELSPIN, cross-relaxation appropriate for minimolecules emulated by locked spins; COSY, correlated spectroscopy; CD, circular dichroism; DMPG, dimyristoyl-*sn*-glycero-3-phosphoglycerol; DQF, double-quantum filtered; FT, Fourier transform; IR infrared; IR-ATR, infrared attenuated total reflection; mrc, mean residue concentration; NOE, nuclear Overhauser effect; NOESY, nuclear Overhauser and exchange spectroscopy; NMR, nuclear magnetic resonance; POPC, 1-palmitoyl-2-oleoyl-*sn*-glycero-3-phosphocholine; ppb, parts per billion; ppm, parts per million; RD, relaxation delay; ROE, rotating frame (transverse) nuclear Overhauser effect; ROESY, rotating frame Overhauser enhancement spectroscopy (2-D CAMELSPIN); RELAY, relayed coherence transfer spectroscopy; SDS, sodium dodecyl sulfate; TFE, 2,2,2-trifluoroethanol; TMS, tetramethylsilane; 1-D, one-dimensional; 2-D, two-dimensional. Standard IUPAC-IUB (1984) three-letter and one-letter symbols for amino acid residues were used throughout.

0006-2960/91/0430-4715$02.50/0

al., 1987), ^{1}H NMR (Zhou & Gibbons, 1986; Renugopalakrishnan et al., 1988), IR/ATR (Erne et al., 1985), FT-IR (Surewicz & Mantsch, 1989), and laser Raman (Rapaka et al., 1987a) studies on dynorphin A-(1–13) and fluorescence energy transfer studies (Schiller, 1983) on Trp^4-dynorphin A-(1–13) and the 17 amino acid peptide. The first contact upon approaching the cell membrane is much more likely to be with the lipid phase than directly with the receptor. In the membrane–water interphase, the peptide assumes a preferred conformation (and orientation) on the basis of its amphiphilicity. The membrane-bound conformation and orientation of the peptide agonist would thus be the one meeting the receptor requirements rather than the random structures in solution. This model could also, for instance, explain the heterogeneity of the opioid receptor types as the membrane-mediated conformation would depend on the exact nature of the lipid environment (Sargent & Schwyzer, 1986).

Schwyzer (1986) has proposed a mechanism of the interaction of dynorphin A-(1–13) with a model membrane. The conformation of the peptide upon binding to the membrane is assumed to be mainly α-helical with the first nine residues forming a helix followed by a randon-coil segment consisting of Pro^{10}–Lys^{13}. Although there has been some experimental observations interpreted as being consistent with the adoption of a helical conformation by dynorphin A-(1–13) after binding to the lipid membrane (Maroun & Mattice, 1981; Erne et al., 1985; Bean et al., 1988; Rapaka et al., 1987b), pharmacological studies indicate that the replacement of the helix-breaking Pro^{10} residue by helix-forming residues results in reduced potency (Turcotte et al., 1984) or decreased selectivity for the κ-opioid receptor (Nakajima et al., 1988). Conversely, a D-Pro^{10}-containing analogue of dynorphin A-(1–11) has been reported (Gairin et al., 1984, 1986) to be more potent and just as selective as U-50,488H, the most κ-selective ligand known. These results indicate that an α-helical conformation does not seem to be a requirement for the κ-opioid receptor.

The hydrophobic moment profile (Eisenberg et al., 1984) and the helix probability profiles for the peptide in aqueous solution and in the presence of anionic detergent (Mattice & Robinson, 1981) suggested to us that the lipid-induced conformation is not α-helical. Regular alternation of hydrophilic and nonpolar side chains in the amino acid sequence from Arg^7 to Lys^{13} indicates the possibility of the formation of an amphiphilic β-strand (Taylor & Kaiser, 1986). However, four-state secondary structure prediction profiles computed with the GOR method (Garnier et al., 1978) predict a reverse turn conformation for the residues Tyr^1, Gly^2, Pro^{10}, and Lys^{11} (Lancaster, 1990). This would interrupt such a β-strand. Taylor (1990) has shown that a peptide model devoid of Pro^{10} has a more pronounced β-strand forming capacity but is less potent in biological assays, thus indicating that only a limited region, if any, of β-structure is beneficial for biological effectiveness. The potential turn at Gly^2 is supported by pharmacological studies on dynorphin analogues indicating a decreased κ potency upon replacement of the Gly^2 residue by several L-amino acids with larger side chains (Bergland et al., 1989) as well as by D-Ala (Chavkin & Goldstein, 1981).

The objective of this study was to further clarify the nature of the membrane-mediated conformation of dynorphin A-(1–13) with the help of circular dichroism (CD) spectropolarimetry and one- and two-dimensional nuclear magnetic resonance (NMR) techniques. The difficulty with directly studying peptide conformation in membranes with NMR arises from line broadening due to the high molecular weight of the aggregates. We therefore sought an organic solvent or micellar system in which the conformation of the peptide would resemble that on the membrane. SDS micelles have been reported to mimic the membrane environment quite well (Wu & Yang, 1981). There is strong evidence supporting the idea that methanol (Yang et al., 1977) and trifluoroethanol (Urry et al., 1971) mimic influences of membranes on peptide conformation (Wu & Yang, 1981). Therefore CD spectropolarimetry was employed to obtain a general indication of the aqueous and membrane-mediated secondary structure of the 13 amino acid peptide. In addition to this, the ability of SDS micelles and organic solvents to mimic the phospholipid environment was compared in order to derive conditions more amenable to a detailed approach employing NMR spectroscopic methods.

Experimental Procedures

CD Studies

Materials. Dynorphin A-(1–13) was synthesized and purified as described previously (Turcotte et al., 1984). Dimyristoyl-*sn*-glycero-3-phosphoglycerol (DMPG) was purchased from Avanti Polar Lipids Inc., Birmingham, AL. Sodium dodecyl sulfate (SDS) was purchased from Bio-Rad (Canada), Mississauga, ON, methanol (HPLC grade) and chloroform were purchased from Caledon Laboratories, Georgetown, ON, Canada, and trifluoroethanol (TFE) from Pierce, Rockford, IL.

Sample Preparation. The lipid suspensions were completely prepared before adding the peptide to the sample. The lipid was dissolved in a mixture of chloroform and methanol (2:1 v/v). The solvent was evaporated with a stream of dry nitrogen, leaving the lipid as film on the walls of a glass test tube. The last traces of solvent were removed into a liquid nitrogen trap by placing the sample under high vacuum for at least 90 min. The lipid film was resuspended in the appropriate solvent (buffer or water) by warming the tube to about 45 °C and vortexing vigorously for about 30 s.

The peptide concentration was checked by UV absorption spectrometry (in water and methanol) where literature data (Sober, 1970) were available. It was determined that the peptide concentration measured in this manner was the same as the concentration calculated on a weight basis. The latter method was used to calculate the concentration in other solvents. The peptide concentrations ranged from 0.16 to 0.26 mM, the SDS detergent-to-peptide ratio was 47, and the DMPG lipid-to-peptide ratio was 11.

Data Acquisition, Data Processing, and Secondary Structure Estimation. Spectra were obtained from an Aviv model 60 DS circular dichroism spectropolarimeter as described earlier (Epand et al., 1986). A 1-mm sample cell was used, and the sample temperature was 25 °C unless stated otherwise. The cell was maintained at constant temperature with a thermostated cell holder. The region from 250 to 190 nm was scanned every 0.5 nm with a bandwidth of 1.5 nm. Four or five scans were averaged. For temperature-dependent studies in methanolic solution, spectra were recorded at 20, 25, 30, 35, 40, and 45 °C. For concentration-dependent studies in methanolic solution, spectra were recorded at 0.16, 0.08, 0.04, 0.02, and 0.01 mM. The cell path length was 1 mm for the first, 2 mm for the second, and 10 mm for the last three concentrations.

Spectra were corrected for the baseline by recording the spectra of the pure solvents under the same conditions and subtracting these from the sample spectra. The corrected data set was multiplied by a constant to obtain the mean residue ellipticity, $[\theta]$. The computer program used for secondary

structure analysis has been described earlier (Epand et al., 1986) and is based on J. T. Yang's program (Chang et al., 1978).

NMR Studies

Additional Materials. Deuterium oxide (^2H_2O), [$^2H_4$]-methanol ($C^2H_3O^2H$), partially deuterated methanol (C^2H_3OH), and perdeuterated acetic acid ($C_2{}^2H_5COO^2H$) were purchased from Merck Sharpe and Dohme (MSD Isotopes), Montreal.

Samples. Studies on the nonlabile protons were performed in CD_3OD; the labile protons were included in studies in CD_3OH (or D_2O and mixtures of H_2O and D_2O with d_6-acetic acid, respectively). Sample volumes and peptide concentrations ranged from 0.35 to 0.7 mL and 5.5 to 40 mM, respectively.

500-MHz NMR

Acquisition Parameters. Spectra were acquired on a Bruker AM-500 spectrometer at the NMR facility of the Department of Chemistry, McMaster University at 500.138 MHz with a 5-mm dual frequency $^1H/^{13}C$ probe. The sample temperature was maintained at 30 ± 1 °C by a Bruker B-VT 1000 variable temperature unit. Temperature-dependent studies were performed at −31, −20, −10, 11, and 30 °C. Chemical shifts are reported in ppm relative to TMS with the residual solvent signals at 3.30 ppm (methanol) and 4.80 ppm (water) as internal references.

Saturation Transfer Experiments. The decoupler power level and the presaturation time were varied separately. The decoupler power level was increased from 2 μW (50 dB) to 6.3 mW (15 dB) in increments of 5 dB with the presaturation time kept constant at 1.0 s. The presaturation time was increased from 0.1 to 3.0 s in increments of 0.1 up to 1.0 s and of 0.5 thereafter with the decoupler power level kept constant at 0.2 mW (30 dB).

Studies of Solvent Exchange. Dynorphin-A-(1–13) was freshly dissolved in perdeuterated methanol (CD_3OD) at −4 and 30 °C, and the decrease of the amide peak areas as a function of time was observed. The individual spectra were scaled to the respective Tyr^1 ε resonance at 6.72 ppm. The time noted was for the middle of the acquisition.

Methanol Titration Experiments. Perdeuterated methanol (CD_3OD) was added in four 0.1-mL increments to the sample containing 6.2 mM dynorphin A-(1–13) in H_2O, pH 2.8 (yielding x_{meth} = 0, 0.09, 0.17, 0.23, and 0.29, respectively). A 140 mM solution of d_6-acetic acid (CD_3COOD) in H_2O, pH 2.8, was added in four 0.1-mL increments to the sample containing 25 mM dynorphin A-(1–13) in CD_3OD (i.e., x_{meth} = 1, 0.67, 0.50, 0.40, and 0.34, respectively).

Two-Dimensional Studies

^1H–^1H COSY (Aue et al., 1976). The absolute value spectra were generated by the standard pulse sequence: RD–$(\pi/2)_{\phi 1}$–t_1–$(\pi/2)_{\phi 2}$–FID$_\phi$, where $\phi 1$, $\phi 2$, and ϕ were the respective phases for phase cycling of the pulse sequence. The 16-step phase cycle consisted of a standard combination of the ν_1 quadrature-detection scheme by echo detection, axial peak suppression, and the CYCLOPS (cyclic ordered phase scheme) procedure for the reduction of quadrature images (Hoult & Richards, 1975). The $\pi/2$ pulse width was 19 μs.

DQF Phase-Sensitive ^1H–^1H COSY. Phase-sensitive COSY experiments were performed with a double-quantum filter (Piantini et al., 1982; Rance et al., 1983). Time-proportional phase incrementation (TPPI) (Drobny et al., 1979; Marion & Wüthrich, 1983) was employed for the implementation of quadrature detection in ν_1. The phase of the first pulse is incremented by 90° for successive t_1 values, while the phase of the second pulse is kept constant. The pulse sequence employed was RD–$(\pi/2)_{\phi 1}$–t_1–$(\pi/2)_{\phi 2}$–τ–$(\pi/2)_{\phi 3}$–FID$_\phi$, where $\phi 1$, $\phi 2$, $\phi 3$, and ϕ are the respective phases for phase cycling of the pulse sequence. The interval τ was set to 3 μs to allow for phase switching between the second and the third pulse. A 16-step phase cycle was utilized. The relaxation and solvent presaturation delay was 2 s. A total of 64 scans were accumulated for each of the 256 FID's containing 2048 data points in F_2 over a spectral width of 4545 Hz. The data were zero filled to 4096 data points in the t_2 dimension and to 2048 data points in the t_1 dimension. Sine-bell window functions were applied to both dimensions before Fourier transformation. Cross sections were taken along F_2 at the F_1 positions of the Gly^2 NH (8.77 ppm), Gly^3 NH (8.24 ppm), Tyr^1 α (4.07 ppm), and Phe^4 α (4.44 ppm) and subjected to inverse Fourier transformation, zero filling to 32K data points, and renewed Fourier transformation. The improved digital resolution was 0.28 Hz/point. The extraction of coupling constants was performed with the antiphase components yielding the active coupling and the in-phase components displaying the passive coupling [Wüthrich (1986), pp 79–85].

Relayed Homonuclear Correlated Spectroscopy (RELAY). The pulse sequence employed was RD–$(\pi/2)_{\phi 1}$–t_1–$(\pi/2)_{\phi 2}$–τ–$(\pi)_{\phi 3}$–τ–$(\pi/2)_{\phi 3}$–FID$_\phi$, where $\phi 1$, $\phi 2$, $\phi 3$, and ϕ are the respective phases for the phase-cycling scheme reported by Hughes et al. (1985). The delay time τ was set to 0.013 s according to the spin-system analysis of Bax and Drobny (1985), resulting in a total mixing time of 0.026 s. A total of 96 scans were accumulated for each of the 256 FID's. All other acquisition parameters were the same as for the respective COSY experiment.

620-MHz NMR

Acquisition Parameters. 620-MHz NMR spectra were recorded on the spectrometer at the NMR Facility for Biomedical Studies, Mellon Institute, Carnegie-Mellon University, Pittsburgh, PA. The spectrometer was equipped with a Varian XL400 console with Varian software 6.1 revision B.

One-Dimensional Spectroscopy. Spectra were acquired at 620.166 MHz over a spectral width of 5200.2 Hz in 30016 data points (2.886-s acquisition time). The sample temperature was 23 °C. Chemical shifts are reported in ppm relative to TMS with the residual CD_2H methanol signal at 3.30 ppm used as an internal reference.

Two-Dimensional NMR Spectroscopy. For the standard COSY experiment, 64 scans were accumulated in blocks of 16 scans for each of the 512 FID's containing 1024 data points in F_2 over a spectral width of 5200 Hz. The $\pi/2$ pulse width was 12.6 μs. Representative COSY and DQF COSY experiments are described in the captions of Figures 7 and 3, respectively. NOESY spectra were recorded on 20 mM dynorphin A-(1–13) in CD_3OH with mixing times, τ_m, of 100 and 500 ms and on 40 mM dynorphin A-(1–13) in CD_3OD with mixing times of 100, 200, 300, 400, and 600 ms by employing the pulse sequence RD–$(\pi/2)$–t_1–$(\pi/2)$–τ_m–$(\pi/2)$–FID. The phase-sensitive experiment described by States et al. (1982) and modified by Varian was employed. A representative NOESY experiment is described in the caption of Figure 7.

Rotating-Frame Overhauser Enhancement Spectroscopy (2-D CAMELSPIN/ROESY). The experiment was performed on 20 mM dynorphin A-(1–13) in CD_3OH. The pulse sequence used was RD–$(\pi/2)_{\phi 1}$–t_1–spin-lock–FID$_\phi$. The relaxation delay was 4 s. The $\pi/2$ pulse was 77.5 μs. The

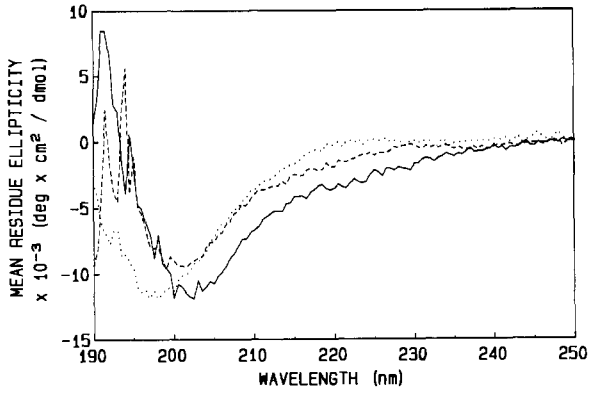

FIGURE 1: Circular dichroism spectra of dynorphin A-(1–13) solutions in water (···), methanol (---), and aqueous DMPG bilayers (—). See Table I for conditions.

Table I: Estimation of the Secondary Structure Fractions of Dynorphin A-(1–13) in Different Solvent Environments from Circular Dichroism[a]

solvent	C_{pep} (mM)	fractions of total			
		α-helix	β-sheet	β-turn	random
water	0.24	0.0	0.44	0.13	0.44
methanol	0.24	0.0	0.60	0.05	0.35
50% methanol	0.24	0.0	0.55	0.04	0.41
8.5 mM SDS	0.21	0.02	0.59	0.0	0.39
TFE	0.19	0.08	0.51	0.0	0.41
30% TFE	0.26	0.0	0.53	0.04	0.43
1.8 mM DMPG[b]	0.16	0.02	0.57	0.0	0.41

[a] The error in secondary structure determination from different preparations of the same sample was estimated at ±0.02. [b] In 10 mM NaH_2PO_4, pH 7.46.

spin-lock was applied for 200 and 500 ms, respectively. A total of 32 scans were accumulated for each of the 256 FID's containing 1024 data points in F_2 over a 5200-Hz spectral width (0.098-s acquisition time). The data were zero filled in both dimensions to 2048 data points. Gaussian window functions were applied to both dimensions before Fourier transformation. The digital resolution was 5.1 Hz/point in both dimensions.

Results and Discussion

CD Studies

The difference in the CD spectra of dynorphin A-(1–13) in aqueous solution and in DMPG bilayers is illustrated in Figure 1, as is the similarity of the latter spectrum to that recorded in methanol. This is also indicated in the estimated secondary structure fractions calculated from the CD spectra (Table I). The correspondence of the results for SDS and DMPG is within the estimated error margin. In the case of methanol and DMPG, the correlation is not as good, but the differences in the values are only slightly greater than the error margin. This is not the case for the comparison of the DMPG and water spectra, which show larger differences (Table I).

Correspondence of the spectrum of the peptide in methanolic solution with that in DMPG bilayers supports the idea that the membrane-mediated conformation of the peptide may be mimicked in this system, which led to the choice of this solvent for NMR studies. Mixed solvents were not employed for NMR investigations, as they would have entailed suppressing two different strong and exchange-broadened solvent signals. 30% TFE mimics the membrane environment better than 100% TFE does. The calculated α-helical content was negligible in all cases (≤4%), except for the system with pure TFE (Table I). Similar results were obtained by Kojro et al. (1987) for CD spectra in water and TFE, respectively. The probable reason for this is that TFE alone is too apolar to resemble the hydrophobic–hydrophilic interphase of a membrane surface.

These results are in stark contrast to those obtained by Maroun and Mattice (1981), who reported a helical content of 5% for dynorphin A-(1–13) in water and 17% in SDS micelles on the basis of the measured ellipticity at 222 nm. Application of the method employed by Maroun and Mattice [originally described by Beychok (1967)] for the estimation of α-helical content to our data yields considerably higher values (3–17% as opposed to 0–8%) in all cases. Although the method of Yang's group (Chang et al., 1978) has been shown to be unsatisfactory in the prediction of β forms (Yang et al., 1986), its estimates of helical content from CD spectra are within ±10% of the helical content established by X-ray crystallography (Yang et al., 1986). Confirmation of Schwyzer's model would require a helical content of 69% (= 9/13). No significant temperature or concentration dependence of the CD spectrum of dynorphin A-(1–13) in methanolic solution could be observed in the temperature and concentration ranges studied (20–45 °C and 0.01–0.16 mM, respectively). These results support the idea that the CD spectra of dynorphin A-(1–13) in a methanolic solution are not influenced by self-aggregation phenomena and demonstrate that the CD spectra do not constitute the equilibrated average of several distinctly different conformations of significant abundance. Consequently, neither the findings of Maroun and Mattice nor our present study can confirm the validity of Schwyzer's model. On the contrary, they indicate that the proposed conformation is improbable.

NMR Studies

Identification of the Amino Acid Spin Systems. Dynorphin A-(1–13)-peptide consists of 15 spin systems. The residues Gly, Leu, Ile, and Lys have unique nonlabile proton spin systems, and the aromatic spin systems of Tyr and Phe are also characteristic. Upon inclusion of labile protons through employing CD_3OH as a solvent, the spin systems of Arg and Pro differ from one another, as do the backbone spin systems of Phe[4] and Tyr[1] (Figure 2).

The nonlabile protons were assigned on the basis of a variety of one- and two-dimensional experiments. The assignments are outlined mainly on spectra obtained from a double-quantum filtered phase-sensitive COSY experiment (Figures 3 and 4). The labile protons were assigned on the basis of 500-MHz COSY and RELAY spectra (Figures 5 and 6), which also resolved ambiguities among the nonlabile protons (Figure 5).

A problem is the multiple existence of a number of identical residues in the peptide. Gly, Leu, and Lys occur twice and Arg is encountered three times. Nevertheless, it was possible to unambiguously assign all but very few of the resonances sequence specifically. These sequence-specific resonance assignments were achieved in the manner recommended by Wüthrich (1986). After identification of the individual spin systems, sequential interresidue NOE connectivities were derived from NOESY spectra in conjunction with COSY spectra (Figure 7).

Coupling constants were determined by analysis of the line splitting in the one-dimensional spectrum (where possible) and from the examination of the 500-MHz DQF phase-sensitive COSY cross sections that had individually been subjected to zero filling in order to achieve adequate digital resolution. As Wüthrich (1986) has pointed out, the apparent separation of antiphase lines is larger than the true separation due to the

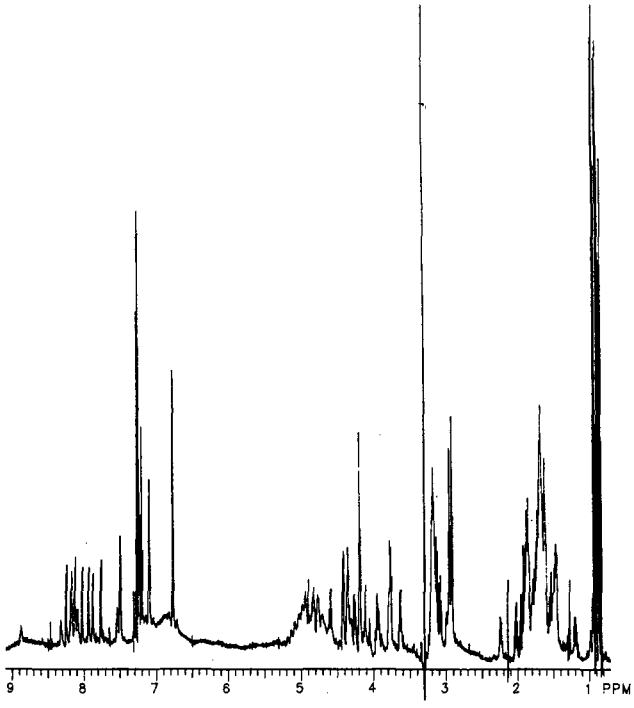

FIGURE 2: 620-MHz one-dimensional spectrum of 20 mM dynorphin A-(1–13) in CD_3OH. A total of 480 scans were accumulated over a spectral width of 5200 Hz in 30016 data points (2.886-s acquisition time). The solvent resonance was suppressed by presaturation during a 1-s delay prior to acquisition. The free induction decay was processed by using a Lorentz-Gauss transformation with $G = e^{t/0.09} \cdot e^{-t^2/0.270}$ for resolution enhancement and was zero filled to 64K before Fourier transformation. The digital resolution is 0.16 Hz/point.

effects of finite line width and limited digital resolution. Therefore the reliability of the exact values determined has to be viewed with caution. The accuracy of the determined coupling constants is estimated at ±0.3 Hz. More complicated multiplets and doublets in regions of considerable overlap were not analyzed at all because of the apparent cancellation of antiphase components.

The alphabetical notation for spin systems within molecules introduced by Pople et al. (1959) was used to describe the spin systems. Only nonlabile protons were considered for the nomenclature, i.e., in all cases except for Tyr^1 and Pro^{10}, a further spin, the backbone amide proton, was included for the experiments in CD_3OH. Under these circumstances, the Arg spin systems also included the ε-guanidino NH, so that two additional spins had to be considered. The individual spin systems are discussed below.

The Ile^8 A_3B_3MPTX Spin System. The Ile^8 δCH_3 resonance was the only triplet in the methyl region (1.0–0.8 ppm, cf. Figure 2) and was therefore easily separated from the other methyl resonances (Ile^8 γCH_3, $Leu^{5,12}$ $\delta,\delta' CH_3$'s).

The Ile^8 γ', γ, β, and γCH_3 resonances were assinged from the DQF-COSY spectrum in Figure 3a. The Ile^8 α-proton resonance could not be assigned on the basis of the COSY spectrum alone, as there were many β–α cross-peaks in the region of interest. It was, however unambiguously identified in the RELAY spectrum in Figure 5. The Ile^8 NH resonance was also assigned on the basis of this RELAY experiment (Figure 6).

The Pro^{10} $AB(MB)EFX$ Spin System. The Pro δ', Pro β, and Pro γ multiplet structures are well separated from other resonances, so that the assignment of the entire spin system is possible on the basis of the DQF-COSY spectrum alone (Figure 3). Noteworthy is the fact that the γ- and γ'-proton resonances could be distinguished (Table II).

The Gly^2 and Gly^3 AX Spin Systems. The α-proton resonances were identified in the COSY spectra (data not shown) and were unambiguously assigned on the basis of their NH–α connectivities (Figure 7). The spin system containing the

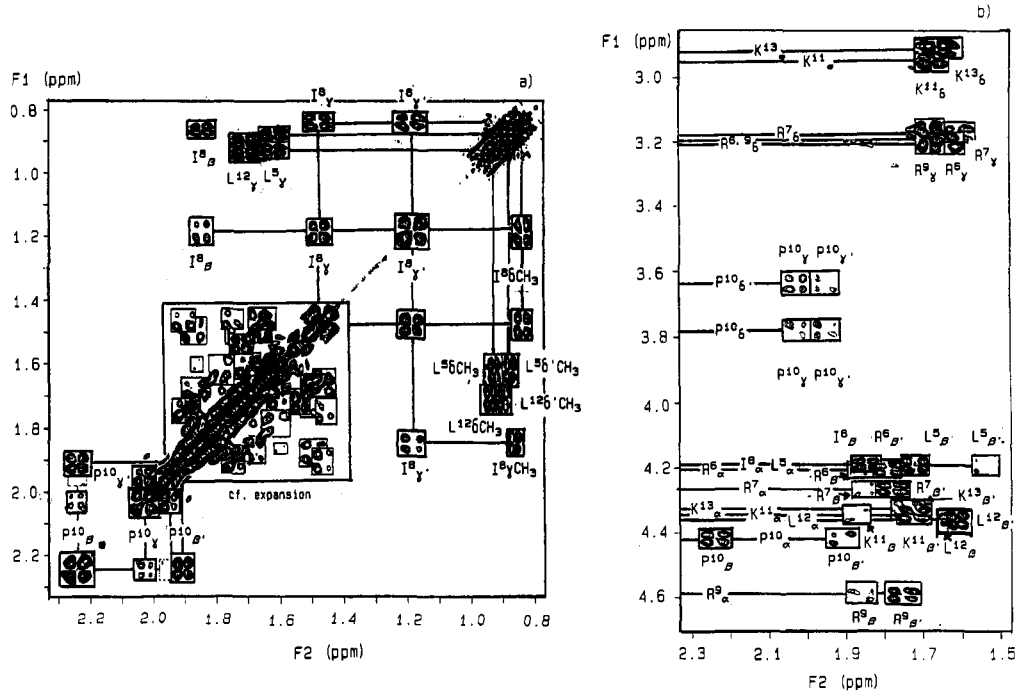

FIGURE 3: 620-MHz double-quantum filtered phase-sensitive COSY spectrum of 40 mM dynorphin A-(1–13) in CD_3OD. The relaxation delay (which was also the period for presaturation of the solvent) was 2 s. A total of 36 scans were accumulated for each of the 256 FID's containing 1024 data points in F_2 over a reduced spectral width of 4200 Hz. Zero filling was applied in both dimensions to 2048 data points. Window functions $[f(t) = e^{-t/3.183} \cdot e^{-t^2/0.072^2}]$ were applied to both dimensions before Fourier transformation. The digital resolution was 4.1 Hz/point in both dimensions. (a) An upfield expansion, the Pro^{10}, Ile^8, Leu^{12}, and Leu^5 connectivities are indicated. The central region was too crowded to be labeled and was expanded further in Figure 4. (b) The α–β connectivity region of the 620-MHz double-quantum filtered phase-sensitive COSY spectrum of 40 mM dynorphin A-(1–13) in CD_3OD. The Pro^{10} δ–γ, Arg δ–γ, and Lys ϵ–δ connectivities are indicated.

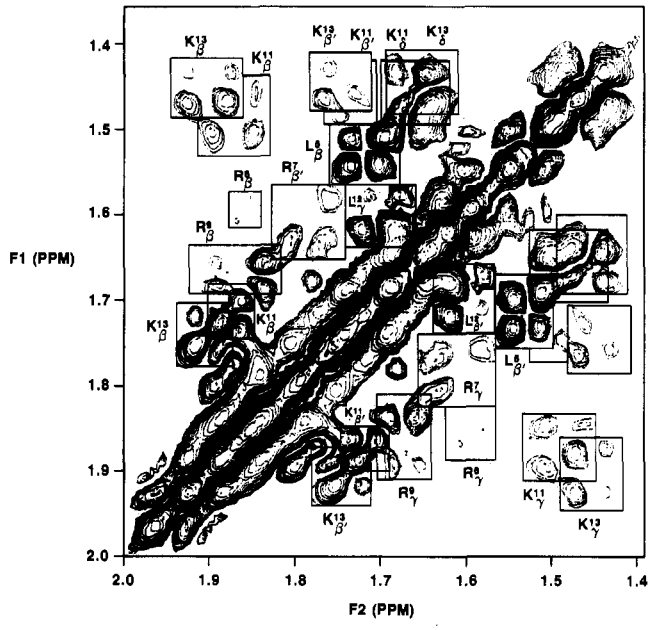

FIGURE 4: Expansion of the central region of Figure 3a.

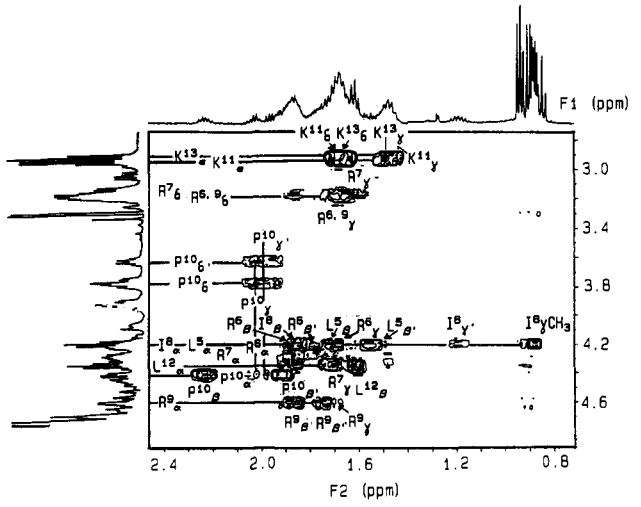

FIGURE 5: Upfield expansion of the 500-MHz ^1H-^1H RELAY experiment on 5.5 mM dynorphin A-(1–13) in CD_3OH. The delay time τ was 0.013 s, resulting in a total mixing time of 0.026 s. A total of 96 scans were accumulated for each of the 256 FID's containing 2048 data points in F_2 over a 4545.455-Hz spectral width. A relaxation delay of 2.0 s was employed. The data were zero filled in the t_1 dimension to 1024 data points. Squared sine-bell window functions were applied to both dimensions before Fourier transformation. The digital resolution was 4.4 Hz/point in both dimensions. The α–β–γ, Arg δ–γ–β, and Lys ϵ–δ–γ connectivities are indicated.

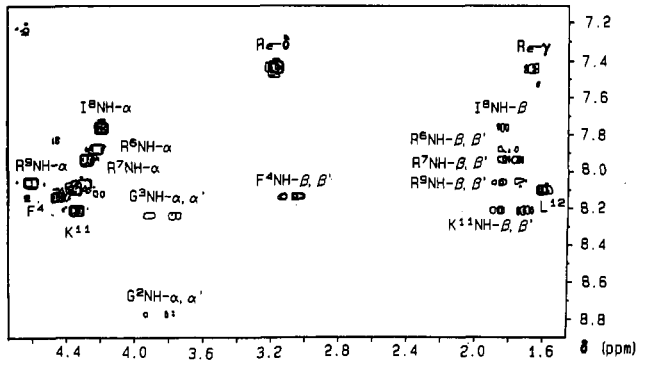

FIGURE 6: NH–α–β connectivities in the RELAY experiment described in the caption of Figure 5. Also indicated are the Arg ϵ–δ–γ connectivities.

Table II: ^1H NMR Assignments of Dynorphin A-(1–13) in Methanolic Solution

	chemical shift δ (±0.01 ppm)				
residue	δ_{NH}[a]	$\delta_{\alpha H}$[a]	$\delta_{\beta H}$	$\delta_{\beta H'}$	other[a]
Tyr[1]		4.10–4.07	3.15	2.99	δ 7.11, ϵ 6.77
Gly[2]	8.86–8.77	3.94	α' 3.77		
Gly[3]	8.30–8.23	3.91	α' 3.76		
Phe[4]	8.17–8.13	4.43	3.15	3.08	δ 7.26, ϵ 7.28, ζ 7.21
Leu[5]	8.17–8.13	4.19	1.73	1.55	γ 1.65, δCH_3 0.94, $\delta' CH_3$ 0.89
Arg[6]	7.88	4.21	1.88	1.80	γ 1.69, δ 3.19, ϵ 7.48–7.43[b]
Arg[7]	7.94	4.27	1.86	1.79	γ 1.62, δ 3.17, ϵ 7.48–7.44[b]
Ile[8]	7.76	4.19	1.85	γ 1.48	γ' 1.19, γCH_3 0.87, δCH_3 0.85
Arg[9]	8.05	4.60	1.88	1.77	γ 1.69, δ 3.19, ϵ 7.51–7.46[b]
Pro[10]		4.42	2.24	1.91	γ 2.03, γ' 1.96, δ 3.78, δ 3.64
Lys[11]	8.25–8.21	4.35	1.84	1.73	γ 1.50, δ 1.68, ϵ 2.95
Leu[12]	8.10	4.37	1.63	1.60	γ 1.71, δCH_3 0.95, δCH_3 0.91
Lys[13]	8.17–8.07	4.33	1.91	1.76	γ 1.47, δ 1.67, ϵ 2.92

[a] During the course of this study (approximately two years), some resonances underwent marked downfield shifts. In these cases, the two extreme values are indicated. [b] Resonances that were not unambiguously assigned.

downfield amide proton was tentatively assigned to Gly[2] in accordance with the findings in aqueous solution (Zhou & Gibbons, 1986). This was confirmed by the sequence-specific resonance assignments. In contrast to the spectrum of the peptide in H_2O, the amide proton signals were broadened, so that individual multiplet components could not be observed. Nevertheless, it was possible to determine the $^3J_{HN\alpha}$ coupling constants from the appropriate cross sections of the DQF phase-sensitive COSY experiment.

The chemical shifts of the amide proton resonances displayed a high degree of fluctuation with time. As these studies were conducted over a period of almost two years, long-term changes in the resonance positions could be observed. The chemical shift of the Gly[2] NH resonance increased from 8.77 via 8.82 to 8.86 ppm, that of the Gly[3] resonance from 8.23 via 8.28 to 8.30 ppm. The change is considered not dramatic enough to be due to a chemical degradation of the sample. An interesting feature derived from Table II is that the difference in the chemical shifts between the geminally coupled protons of the Gly residues is relatively large in our studies, resulting in the observation of AX systems as opposed to the strongly coupled AB systems obtained for the peptide in water (Zhou & Gibbons, 1986).

The Tyr[1] and Phe[4] Backbone AMX and Aromatic Spin Systems. The Phe[4] AA'BB'C aromatic spin system was difficult to disseminate because of the strong coupling involved in the Phe ring, which resulted in a complicated appearance in the one- and two-dimensional spectra. The upfield triplet was assigned to the ζ-proton as the line intensities indicated that this was the only signal arising from a single proton. The two ϵ-protons were expected to give rise to a single triplet of double intensity due to proton exchange by interconversion through 180° ring flips (Jardetzky & Roberts, 1981). This was located at 7.28 ppm. On the basis of the same argument, the δ-protons are expected to give rise to a doublet of double intensity. Such a doublet was identified at 7.26 ppm. The only two-dimensional experiment that yielded resolved cross-peaks amenable to connectivity analysis was the DQF-

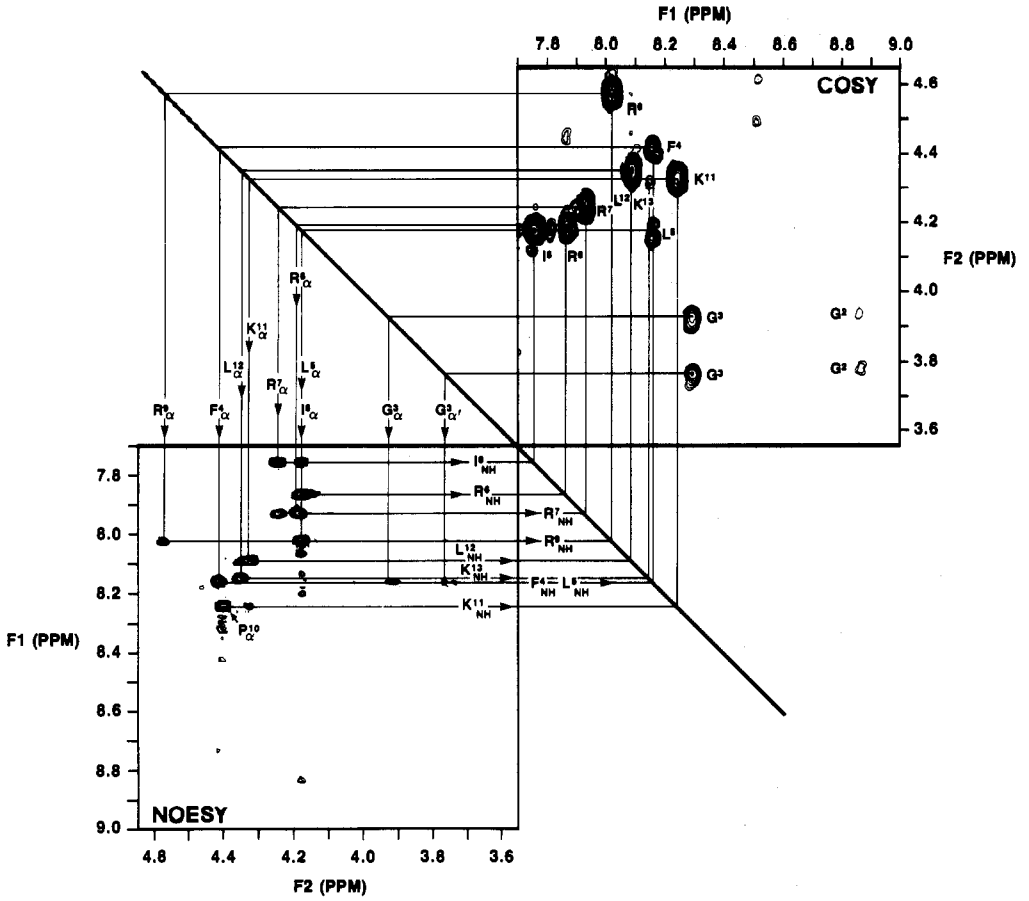

FIGURE 7: Combined COSY (top right) and NOESY (bottom left) connectivity diagram (Wüthrich, 1986) for sequential assignments via NOE's between α-protons and the amide protons of the following residue, $\alpha N(i,i+1)$. The spectra were recorded on 20 mM dynorphin A-(1–13) in CD_3OH. For the COSY spectrum, 80 scans were accumulated for each of the 512 FID's containing 1024 data points. For the NOESY spectrum, 40 scans were accumulated for each of the 256 FID's containing 1024 data points in F_2. The mixing time in the NOESY experiment was 500 ms. In both cases, a relaxation delay of 1.5 s was employed and the data were zero filled to 2048 data points in both dimensions. Pseudo-sine-bell window functions were applied to both COSY dimensions, and Gaussian window functions were applied to both NOESY dimensions before Fourier transformation. For both experiments, the digital resolution was 5.1 Hz/point in both dimensions. Only positive contour levels, i.e., negative NOE's, are plotted in the case of the NOESY experiment. The COSY expansion was plotted in exactly the same limits as the NOESY spectrum [as recommended by Wüthrich (1986)], and the COSY mirror image was created photomechanically to fit into the diagram.

COSY spectrum. The connectivities detected agreed with the above assignments.

The Tyr^1 AA′XX′ aromatic spin system was readily assigned. The broadened appearance of the Tyr δ-doublet as compared to the Tyr ϵ-doublet is attributed to the different time scales defined by the chemical shift differences of the protons undergoing interconversion. In the rigid residue, the δ-proton resonances are usually much further apart than the ϵ-proton resonances and will thus define a much faster time scale (Wüthrich, 1986). Thus, the same interconversion frequency for δ- and ϵ-protons resulted in an exchange regime that is slower on the time scale defined by the δ-protons than on the ϵ-proton time scale.

The β-proton resonances of the aromatic residues are shifted downfield in comparison with other β-proton resonances (Wüthrich, 1986), which facilitates recognition of the backbone spin systems. The cross-peaks connecting α- and β-protons are separated distinctly from all other connectivities. As the labile amino protons of Tyr^1 could not be observed due to fast exchange with the solvent, the Phe^4 backbone spin system was easily distinguished from the Tyr^1 system by the observation of NH–α connectivities in a ^{1}H–^{1}H COSY spectrum of dynorphin A-(1–13) in CD_3OH. The unambiguous assignment of the Phe^4 amide proton was achieved by observing the NH–α–β RELAY connectivities in the RELAY spectrum in Figure 6. The Tyr^1 α resonance was not well resolved in either

Table III: Spin–Spin Coupling Constants of Dynorphin A-(1–13) in Methanolic Solution

	coupling constants ^nJ (±0.3 Hz)			
residue	$^3J_{HN\alpha}$	$^3J_{\alpha\beta}$	$^3J_{\alpha\beta'}$	other
Tyr^1		8.4	8.5	$^2J_{\beta\beta}$ −14.9
Gly^2	7.5			$^3J_{HN\alpha'}$ 6.9, $^2J_{\alpha\alpha'}$ −16.8
Gly^3	6.4			$^3J_{HN\alpha}$ 5.9, $^2J_{\alpha\alpha'}$ −16.7
Phe^4	7.1	6.2	8.6	$^2J_{\beta\beta'}$ −14.3
Leu^5		10.1	4.9	$^3J_{\gamma\delta}$ 6.6, $^3J_{\gamma\delta'}$ 6.5
Arg^6	6.6			
Arg^7	7.0	5.3	9.1	
Ile^8	8.1	7.5		$^3J_{\beta\gamma'}$ 9.0, $^3J_{\beta\gamma CH3}$ 6.8, $^3J_{\gamma\delta CH3}$ 7.8, $^3J_{\gamma\delta' CH3}$ 7.5
Arg^9	7.2	6.1	8.1	
Pro^{10}		8.5	5.6	$^3J_{\gamma\delta}$ 6.8, $^3J_{\gamma\delta'}$ 6.3, $^3J_{\gamma'\delta}$ 6.5, $^3J_{\gamma'\delta'}$ 6.5, $^2J_{\delta\delta'}$ −10.2
Lys^{11}	7.6	5.4	8.9	
Leu^{12}	7.5			$^3J_{\gamma\delta}$ 6.5, $^3J_{\gamma\delta'}$ 6.5
Lys^{13}				

CD_3OH or CD_3OD and was shifted significantly upfield (Table II) compared to the aqueous solution of the peptide (Zhou & Gibbons, 1986).

The coupling constants of Phe^4 and Tyr^1 listed in Table III were all determined from cross sections of the DQF phase-sensitive COSY spectrum on 20 mM dynorphin A-(1–13) in CD_3OH as described above.

The Leu^5 and Leu^{12} A_3B_3MNOX Spin Systems. The γ–δ connectivities were easily recognizable (Figure 3a). The δCH_3

resonances at 0.89 and 0.94 ppm displayed connectivities to a signal at 1.65 ppm, thus assigning the latter to a γCH resonance. The other δCH_3 resonances displayed connectivities to peaks further downfield (1.71 ppm), so that two separate γ,δ,δ' systems could be distinguished. The Leu α–β connectivities were initially assigned (Figure 3b) on the basis of their upfield β-proton resonances (Wüthrich, 1986). The NH–α–β RELAY connectivities lead to the assignment of the amide protons (Figure 6), which were later confirmed by sequence-specific resonance assignments (Figure 7). Assignment of the Leu[12] spin system was supported by an appropriate cross section of the 500-MHz RELAY experiment shown in Figure 5. In the 500-MHz DQF-COSY spectrum on 28 mM dynorphin in CD_3OD, a connectivity was detected between a resonance at 1.55 ppm (assigned to Leu[5]–β') and two resonances at 1.73 (Leu[5]–β) and 1.65 ppm (Leu[5]–γ), respectively.

The Lys[11] and Lys[13] $A_2(K_2T_2)MPX$ Spin Systems. The most characteristic peaks were the ϵCH_2 signals at 2.95 and 2.92 ppm, respectively (Wüthrich, 1986). Connectivities in the COSY (Figure 3b) and RELAY (Figure 5) experiments allowed the assignment of the δ- and γCH_2 proton signals. The β and β' resonances were assigned on the basis of the respective connectivities to the γ-protons (Figure 4). One α-proton, which was subsequently assigned to Lys[11] (cf. sequence-specific assignments), displayed easily detectable β and β' connectivities (Figure 3b). The other α-proton resonance (Lys[13]) could not be assigned in a straightforward manner. It was tentatively assigned to a position slightly upfield from Lys[11] α on the basis of the integration of the one-dimensional spectrum and a weak cross-peak in the COSY spectrum. This was confirmed by the sequence-specific assignments and the corresponding NH–α COSY connectivity. The problem arose from the broadened nature of the Lys[13] α resonance and the consequent low intensity of the corresponding cross-peaks. No coupling constants could be determined for the Lys[13] spin system.

The Lys[13] amide proton resonance line exhibited a considerable susceptibility to changes in its chemical shift position as was observed through comparison of the different COSY spectra (Lancaster, 1990).

Arg[6], Arg[7], and Arg[9]. The Arg[6], Arg[7], and Arg[9] $A_2(T_2)$-MPX spin systems possess characteristic ϵNH resonances that were found at approximately 7.49 ppm. Connectivities obtained from COSY (Figure 3b) and RELAY (Figure 6) experiments yield the positions of the δ- and γ-methylene proton resonances, respectively. The β–γ connectivities were difficult to identify because all of the respective resonances were located in the extremely dense region between 1.9 and 1.6 ppm (Figure 2). Nevertheless, connectivities were established between the γ-protons and at least one of the β-protons of each residue (Figure 3a). The recognition of β–α (Figure 3b) connectivities as well as NH–α–β RELAY connectivities (Figure 6) and sequence-specific assignments (Figure 7) in all three cases led to complete assignments.

Sequence-Specific Assignments. Sequence-specific assignments were obtained with the aid of NOESY spectra and the respective COSY spectra. Both intraresidue and sequential through-space connectivities are established in the α-NH region of NOESY spectra. They can be distinguished only by comparison of the NOESY spectra with COSY spectra acquired under the same conditions (Wüthrich, 1986). This is demonstrated in Figure 7. Some of the cross-peaks in the NOESY spectrum were intraresidue connectivities and were identified by comparison with the accompanying COSY spectrum. The $\alpha(i)$–NH(i+1) connectivities are indicated and can be followed from the amino terminus to the carboxy terminus of the molecule. No connectivities could be detected between Tyr[1] α and Gly[2] NH. The one-dimensional spectrum indicated that both peaks were broadened considerably, so that the respective NOESY cross-peak was not likely to be observed. The Gly[2] α–Gly[3] NH connectivity was also missing. No satisfying explanation for this has been found. These missing connectivities do not present a problem as the assignment of the Tyr[1] backbone spin system was unambiguous and because the ensuing assignment of Gly[3] spin system rendered the identification of the Gly[2] spin system equally obvious.

The Gly[3] α–Phe[4] NH connectivity is indicated. As the amide resonances of Phe[4] and Leu[5] overlapped (cf. COSY), no distinction could be made as to whether the NOESY cross-peak at the position of the Phe[4] α resonance was an intraresidue (Phe[4] α–Phe[4] NH) or sequential cross-peak (Phe[4] α–Leu[5] NH) or both. From the Leu[5] α-proton resonance, the connectivity pattern could be followed through via Arg[6] NH, Arg[6] α, Arg[7] NH, Arg[7] α, Ile[8] NH, Ile[8] α, and Arg[9] NH to the Arg[8] α resonance, where the $\alpha(i)$–NH(i+1) connectivity pattern was interrupted. This is due to the absence of an amide proton from the Pro[10] residue.

The Arg[9] α–Pro[10] δ' and Arg[9] α–Pro[10] δ connectivities were observed, thus further confirming the sequence-specific assignments and also indicating a trans Arg[9]–Pro[10] peptide bond [This is independently indicated by the ^{13}C chemical shifts for the Pro[10] residue (Lancaster, 1990)]. The $\alpha(i)$–NH(i+1) connectivity pattern was reinitiated at the position of the Pro[10] α resonance and continued via Lys[11] NH, Lys[11] α, Leu[12] NH, Leu[12] α, and Lys[13] NH to the Lys[13] α resonance. The Lys[13] α–NH COSY cross-peak was very weak compared to the others. This was due to a broadened amide resonance of the carboxy-terminal residue.

In summary, although the $\alpha(i)$–NH(i+1) connectivity map did not include the first two residues of the peptide, the whole molecule has been sequence-specifically assigned on the basis of the spectra shown in Figure 7. The assignments are summarized in Table II.

Conformational Studies

ROESY or 2-D CAMELSPIN Spectra. The relative size of the intraresidue ^1H–^1H distance $d_{N\alpha}(i,i)$ and the sequential distance $d_{\alpha N}(i,i+1)$ can be deduced from the intensity of the respective nuclear Overhauser effects, as long as the respective rotational correlation times do not differ too much. The rotating-frame NOE (ROE) is far less sensitive to τ_c than the laboratory-frame NOE (Neuhaus & Williamson, 1989). The ROE is therefore a better indicator of relative distances than the conventional NOE. The ratio of the intensity of the sequential ROE arising from $d_{\alpha N}(i,i+1)$ to that of the intraresidue ROE corresponding to $d_{N\alpha}(i,i)$ differs markedly for different secondary structures. Three intraresidue ROE's were identified in the NH–α connectivity region of a 2-D CAMELSPIN/ROESY experiment with a mixing time of 200 ms on 20 mM dynorphin A-(1–13) in CD_3OH. They were assigned to the residues Arg[7], Ile[8], and Arg[9] and were consistently markedly weaker than the corresponding sequential ROE's (the intraresidue Arg[9] ROE was compared to the sequential Ile[8] α–Arg[9] NH ROE due to the nonexistence of a Pro[10] NH proton). As the intraresidue ROE would be approximately five times stronger than the sequential ROE in the case of a helical conformation, this was a clear indication for the absence of a helical structure. Thus the ratio of the intensities of sequential to intraresidue ROE's indicate that the backbone conformation in this central part of the molecule (residues 7–9) is a mixture of β-strand and extended structures.

Vicinal $^3J_{HN\alpha}$ Spin–Spin Coupling Constants. Rigid helical structures [ϕ(α-helix) = .57°, ϕ (3_{10}-helix) = −60° (IUPAC-IUB, 1970)] give rise to small $^3J_{HN\alpha}$ values of approximately 4 Hz, whereas antiparallel (ϕ = −139°) and parallel β-sheets (ϕ = −119°) result in large $^3J_{HN\alpha}$ coupling constants of approximately 9 Hz (Pardi et al., 1984). Small coupling constants have been employed as an indication of α-helical structure in methanolic solutions of the 26 amino acid residue linear peptide δ-hemolysin (Tappin et al., 1988).

Very often, many nearly energetically equivalent conformations of linear oligopeptides are in rapid equilibrium. The lack of temperature dependence in our CD studies demonstrates that if there is an equilibrium among several conformations, none of the predominant conformations have a high content of secondary structure. At the same time the peptide is small and therefore is unlikely to adopt a single rigid conformation in solution. We would like to suggest that there is an equilibrium among peptide conformations that are not distinctly different from each other. Thus, the observed values for $^3J_{HN\alpha}$ may not correspond to a rigid angle θ, but rather to an average over a range of values for θ. This is more and more likely to be the case, the closer the $^3J_{HN\alpha}$ values are to 7.5 Hz (Kessler et al., 1985). Indeed, none of the $^3J_{HN\alpha}$ coupling constants of the non-glycine residues deviated more than 1 Hz from this mean value (Table III). It was therefore concluded that the vicinal coupling constants $^3J_{HN\alpha}$ were consistent both with an extended and a "random" structure of the peptide.

$^3J\alpha\beta$ Coupling Constants and Side-Chain Rotamer Analysis. The NMR spectrum is assumed to be an average of the spectra of each of the three minimum energy rotamers about the C_α–C_β bond, weighted by the relative populations (Jardetzky & Roberts, 1981). Assignment of the two individual β-proton resonances is a prerequisite for rotamer analysis. The average coupling constant observed for the two individual β-protons is

$$^3J_{\alpha\beta1} = f_a \cdot {}^3J_g + f_b \cdot {}^3J_t + f_c \cdot {}^3J_g$$

$$^3J_{\alpha\beta2} = f_a \cdot {}^3J_t + f_b \cdot {}^3J_g + f_c \cdot {}^3J_g$$

where f_a, f_b, and f_c are the fractional populations of the three rotamers with $f_a + f_b + f_c = 1$. These are denoted a for χ_1 = −60° (IUPAC-IUB, 1970), b for χ_1 = 180°, and c for χ_1 = 60°. J_g and J_t are the coupling constants for the relationship between the α-proton and each of the β-protons, which are in gauche (θ = 60°) or trans (θ = 180°) arrangement to the α-proton, respectively. Values for ^3J_t (13.6 Hz) and ^3J_g (2.6 Hz) proposed by Pachler (1964) from the analysis of six independent model systems have been widely used (Bystrov, 1976; Zhou & Gibbons, 1986).

For given values of ^3J_g and ^3J_t, determination of $^3J_{\alpha\beta1}$ and $^3J_{\alpha\beta2}$ yields f_a, f_b, and f_c (cf. Table IV).

A problem is the lack of stereospecific assignments for the rectus (pro-*R*) and sinister (pro-*S*) β-methylene protons. The downfield β-proton was arbitrarily assigned to β_1, the upfield β-proton (β') to β_2. The rotamer populations (Table IV) can therefore be reversed for some or all of the residues except Ile^8. In the case of Ile^8, the second β-proton is replaced by the γ-methyl group, so that only one rotamer population could be determined. No single rotamer population exceeded 70% [the highest was 68% for f_b (Leu^5)].

Temperature Dependence of Amide Proton Chemical Shifts. Amide protons involved in intramolecular hydrogen bonds or otherwise shielded from the solvent will not only have different chemical shifts from the solvent-exposed amide protons but also show a decreased temperature sensitivity of their chemical shifts (Kopple et al., 1969a,b; Ohnishi & Urry, 1969). This is ascribed to an increase in the fraction of the amide protons that are accessible to the solvent (Jardetzky & Roberts, 1981).

Table IV: Relative Populations of the Side-Chain Rotamers of Dynorphin A-(1–13) in Methanolic Solution

residue	$^3J_{\alpha\beta} \equiv {}^3J_{\alpha\beta1}$	$^3J_{\alpha\beta'} \equiv {}^3J_{\alpha\beta2}$	f_a[a]	f_b[a]	f_c[a]
Tyr^1	8.4	8.5	0.54	0.53	−0.06
Phe^4	6.2	8.6	0.55	0.33	0.13
Leu^5	10.1	4.9	0.21	0.68	0.11
Arg^7	5.3	9.1	0.59	0.25	0.16
Ile^8	7.5		[b]	0.43	[b]
Arg^9	6.1	8.1	0.50	0.32	0.18
Lys^{11}	5.4	8.9	0.57	0.25	0.17

[a] $f_a = ({}^3J_{\alpha\beta2} - {}^3J_g)/({}^3J_t - {}^3J_g)$, $f_b = ({}^3J_{\alpha\beta1} - {}^3J_g)/({}^3J_t - {}^3J_g)$, and $f_c = 1 - (f_a + f_b)$. [b] As Ile^8 has only one β-proton, only one rotamer population could be determined.

Temperature-dependent studies were performed on the sample containing 20 mM dynorphin-A-(1–13) in CD_3OH. Proceeding to lower temperatures, substantial line broadening was observed because of loss in rotational mobility (i.e., longer correlation times τ_c) and concomitant reduction of the spin–spin relaxation time (i.e., smaller T_2's). The chemical shifts of the resonances not individually resolved were estimated by assigning the value of the resultant peak maximum to them. The error made did not seem significant. The Gly^3 resonance was shifted below the neighboring peaks and could not be monitored.

The temperature coefficients ($\Delta\delta/\Delta T$) for all backbone amide protons except Gly^3 were determined by linear regression and were all in the range of −6 ± 2 ppb/°C. These results were comparable to those for solvent accessible protons in dimethyl sulfoxide (−6 ppb/°C) and considerably larger in magnitude than the temperature coefficients for solvent-shielded or hydrogen-bonded amide protons in aqueous solution (Zhou & Gibbons, 1986), where $|\Delta\delta/\Delta T| \leq 3.0$ ppb/°C (Kopple et al., 1969a,b; Ohnishi & Urry, 1969). Consequently, the temperature-dependent studies give an indication neither of significant amide proton involvement in intramolecular hydrogen bonding nor of solvent inaccessibility of the amide protons for steric reasons.

Solvent Exchange of Amide Protons. The proton exchange rates of individual backbone NH groups with the solvent indicate whether an amide proton is hydrogen bonded or not. A slow exchange is indicative of hydrogen bonding, while rapid exchange suggests a noninvolvement in hydrogen bonding. If sequence-specific assignments have been made, then the various secondary structure types can be distinguished (Wüthrich, 1986). In a helix, all the backbone amide protons are hydrogen bonded except for those of the first three (in a 3_{10}-helix) or four (in an α-helix) residues.

Saturation transfer experiments were not successful in giving information on dissimilar exchange rates of the backbone amide protons with the solvent. None of the amide signals displayed saturation effects. Saturation transfer can be observed if the longitudinal relaxation time of a labile proton is long compared to its exchange lifetime [$>10^{-3}$ min, Wüthrich (1986), p 38]. If the exchange lifetimes are considerably longer ($>10^{-1}$ min), these signals are unaffected by selective saturation of the solvent signal. If all amide proton resonances behave in the same way, this slower exchange is unlikely to be caused by hydrogen bonding. It is more probable that this slower exchange can be attributed to the lack of acid or base catalysis of the exchange reaction in methanolic solution. Failure to exhibit saturation transfer effects can therefore not

be taken as direct evidence for hydrogen bonding of the amide protons.

Observing the decrease in amide peak integrals after dissolving the peptide in perdeuterated methanol (CD_3OD) was more successful in monitoring solvent exchange. As expected, the exchange lifetimes were considerably longer at −4 °C than at 30 °C, where the slowest measured exchange rate was only a third of the fastest detectable rate. A sufficient number of data points were available for crude estimates of the exchange rates for five amide resonances (Arg^6, Arg^7, Ile^8, Arg^9, and Lys^{11}). The glycine amide resonances exchanged too fast to be detected in this experimental setup. This was not unusual and has also been observed by others (Zhou & Gibbons, 1986) in analogous experiments. The other four amide resonances (Phe^4, Leu^5, Leu^{12}, and Lys^{13}) apparently overlapped and could only be measured together. The appearance and the position of this resultant peak did change, however, indicating that the four partially overlapping resonances exchange with different rates.

The apparent first-order exchange rate constants $k' = -\ln (I/I_0)/t$ (with I/I_0 being the integrated intensity at the time t relative to the initial integrated intensity) were determined from the slopes ($= -k'$) in a ln (I/I_0) vs t diagram and ranged from $2.5 \cdot 10^{-3}$ min^{-1} (Ile^8) to $8.9 \cdot 10^{-3}$ min^{-1} (Arg^7). The values are not claimed to be very accurate, but it was apparent that they did not differ significantly enough (i.e., by an order of magnitude) to account for differential inaccessibility of the respective amide protons to be due to hydrogen bonding.

Water–Methanol Titration Experiments. Studies on the solvent composition dependence of peptide NMR spectra were originally introduced (Pitner & Urry, 1972; Kumar & Urry, 1973) as a method for determining whether amide protons are "exposed to" or "shielded from" the solvent either sterically or through the formation of intramolecular hydrogen bonds. This interpretation is, however, only straightforward if no change in the backbone conformation of the peptide is incurred (Higashijima et al., 1979).

Although COSY spectra were recorded at three different mole fractions of methanol ($x_{meth} = 0, 0.34, 1.0$), not all amide proton resonances could be identified unequivocally in all spectra. Consequently, not all of the amide proton resonances could be followed through all stages of the titration experiments. The Gly^2, Gly^3, Phe^4, Ile^8, Arg^9, and Lys^{11} resonances could be assigned unambiguously at $x_{meth} = 0.34$.

With respect to the chemical shifts in water ($x_{meth} = 0$), all resonances initially experienced an upfield shift upon addition of methanol. This was expected as addition of the less polar solvent (methanol) causes less deshielding of the protons, inducing upfield shifts. The magnitude of this effect was very different for the individual amide resonances, most noticeable was the large shift to higher field incurred by the Arg^9 NH resonance. Further addition of methanol resulted in progressive upfield shifts.

The solvent composition dependences were, however, not monotonic for Gly^2 NH, Gly^3 NH, and Phe^4 NH. If a conformational change is induced, changes in hydrogen bonding will be reflected in alterations of the electron densities of amide groups (Schwyzer & Ludescher, 1969; Llinas & Klein, 1975) and manifest themselves in a downfield shift upon hydrogen-bond formation. This provides a good explanation for the eventual increase in the chemical shifts of Gly^2 NH, Gly^3 NH, and Phe^4 NH at higher mole fractions of methanol (Figure 8).

It is interesting to note that these eventual downfield shifts could be observed only for the three amide protons nearest to the amino terminus. This could be an indication of a major conformational rearrangement in the N-terminal region of the peptide upon a change of the solvent environment from water to methanol. However, such conclusions should be viewed with caution as the data set is incomplete. Another indication for a change in conformation was given by significant solvent dependences of the α-protons. Particularly striking was the effect on Phe^4 α (Lancaster, 1990). A slight downfield shift of the Leu^5 δCH_3 resonances could be due to a minor change in the ring current effect arising from the Phe^4 ring, but this change was minute compared to the ring current effects observed in folded proteins (McDonald & Phillips, 1967).

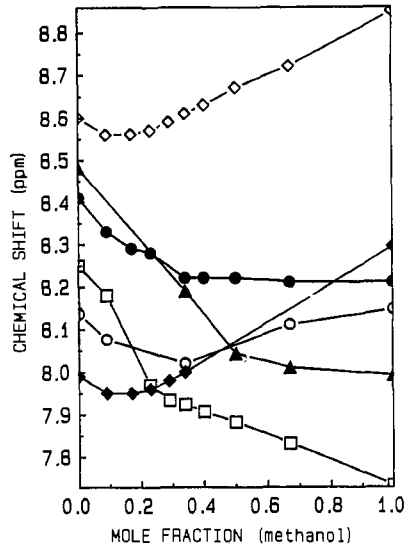

FIGURE 8: Chemical shifts of the backbone amide protons of dynorphin A-(1–13) in mixtures of water and methanol at different mole fractions of CD_3OD: Gly^2 (unfilled diamonds); Gly^3 (filled diamonds); Lys^{11} (filled circles); Phe^4 (unfilled circles); Arg^9 (filled triangles); and Ile^8 (unfilled squares). Not all resonances could be monitored over the whole titration range.

CONCLUSION

CD spectra of dynorphin A-(1–13) in dispersions of DMPG bilayers indicated that dynorphin A-(1–13) is unlikely to adopt an α-helical conformation upon binding to a negatively charged membrane surface. They also indicated that the aqueous–membraneous interphase may be mimicked by methanol.

The NMR resonances of all of the nonlabile backbone amide protons in the ^1H NMR spectrum of dynorphin A-(1–13)-peptide in methanolic solution were unambiguously assigned. $^3J_{HN\alpha}$ coupling constants were not indicative of rigid ϕ angles but seemed to represent averages over rotational states of the backbone. The values were, however, consistent with an extended structure. The observation of sequential α–NH ROE's stronger than the corresponding intraresidue NH–α ROE's for Arg^7, Ile^8, and Arg^9 indicated a β-strand or an extended conformation for this part of the molecule. Temperature dependences and, where determined, deuterium exchange rates of the backbone amide protons demonstrated that the amide protons were all solvent accessible. χ_1 side-chain rotamer analysis revealed no single preferred conformation of the side chains.

The existence of a reverse turn at Pro^{10}, as predicted by the GOR method, can not be proven with our spectroscopic data. This is not surprising since the identification of turns is less reliable than the identification of other structures both by CD (Chang et al., 1986) and NMR spectroscopy [Wüthrich (1986), p 166]. However, in a review on FT-IR, Surewicz and Mantsch (1988) have pointed out that amide I bands around

1665 cm^{-1} are regarded as being highly characteristic of turns. The IR spectrum of dynorphin A-(1–13) on a POPC membrane surface (Erne et al., 1985) displays an amide I band at 1665 cm^{-1}. Originally, the authors took this as evidence for the formation of a short helix consisting of six to nine amino acid residues. Surewicz and Mantsch (1988), however, state than an α-helical segment would exhibit an amide I band between approximately 1650 and 1658 cm^{-1}. Therefore, the aforementioned IR-ATR spectrum could be interpreted as an indication for the occurrence of turns, most probably at Gly^2 and Pro^{10}.

Acknowledgments

The sample preparation and acquisition of the CD spectrum of dynorphin in the presence of DMPG bilayers was performed by Dr. R. F. Epand. Roy Lancaster wishes to acknowledge financial and administrative support by the Tübingen–McMaster exchange program.

Registry No. MeOH, 67-56-1; dynorphin A-(1–13)-peptide, 72957-38-1.

References

Aue, W. P., Bartholdi, E., & Ernst, R. R. (1976) *J. Chem. Phys. 64*, 2229–2246.

Bax, A., & Drobny, G. (1985) *J. Magn. Reson. 61*, 306–320.

Bean, J. W., Erne, D., Sargent, D. F., & Schwyzer, R. (1986) in *Peptides: Chemistry and Biology. Proceedings of the Tenth American Peptide Symposium 1987* (Marshall, G. R., Ed.) pp 328–329, Escom Science, Leiden, The Netherlands.

Bergland, S. S., DeLander, G. E., Murray, T. F., & Lovett, J. A. (1989) in *Eleventh American Peptide Symposium Abstracts*, P-247, The Salk Institute and University of California, San Diego, La Jolla, California.

Beychok, S. (1967) in *Poly-α-Amino Acids. Protein Models for Conformational Studies* (Fasman, G. D., Ed.) Vol. 1, pp 293–337, Marcel Dekker Inc., New York.

Botticelli, L. J., Cox, B. M., & Goldstein, A. (1981) *Proc. Natl. Acad. Sci. U.S.A. 78*, 7783–7786.

Bystrov, V. F. (1976) *Prog. Nucl. Magn. Reson. Spectrosc. 10*, 41–81.

Chang, C. T., Wu, C.-S. C., & Yang, J. T. (1978) *Anal. Biochem. 91*, 13–31.

Chavkin, C., & Goldstein, A. (1981) *Proc. Natl. Acad. Sci. U.S.A. 78*, 6543–6547.

Chavkin, C., & James, I. F. (1982) *Science 215*, 413–415.

Drobny, G., Pines, A., Sinton, S., Weitekamp, D. P., & Wemmer, D. (1979) *Faraday Symp. Chem. Soc. 13*, 49–55.

Eisenberg, D., Weiss, R. M., & Terwilliger, T. C. (1984) *Proc. Natl. Acad. Sci. U.S.A. 81*, 140–144.

Epand, R. M., Epand, R. F., Orlowski, R. C., Seyler, J. K., & Colescott, R. L. (1986) *Biochemistry 25*, 1964–1968.

Erne, D., Sargent, D. F., & Schwyzer, R. (1985) *Biochemistry 24*, 4261–4263.

Gairin, J. E., Gouarderes, C., Mazarguil, H., Alvinerie, P., & Cros, J. (1984) *Eur. J. Pharmacol. 106*, 457–458.

Gairin, J. E., Jomary, C., Pradayrol, L., Cros, J., & Meunier, J.-C. (1986) *Biochem. Biophys. Res. Commun. 134*, 1142–1150.

Garnier, J., Osguthorpe, D. J., & Robson, B. (1978) *J. Mol. Biol. 120*, 97–120.

Goldstein, A., Tachibana, S., Lowney, L. I., Hunkapiller, M., & Hood, L. (1979) *Proc. Natl. Acad. Sci. U.S.A. 76*, 6666–6670.

Goldstein, A., Fischli, W., Lowney, L. I., Hunkapiller, M., & Hood, L. (1981) *Proc. Natl. Acad. Sci. U.S.A. 78*, 7219–7223.

Higashijima, T., Kobayashi, J., Nagai, U., & Miyazawa, T. (1979) *Eur. J. Biochem. 97*, 43–57.

Hoult, D. J., & Richards, R. E. (1975) *Proc. R. Soc. London, A 344*, 311–340.

Hughes, D. W., Bell, R. A., Neilson, T., & Bain, A. D. (1985) *Can. J. Chem. 63*, 3133–3139.

IUPAC-IUB Commission on Biochemical Nomenclature (1970) *Biochemistry 9*, 3471–3479.

IUPAC-IUB Joint Commission on Biochemical Nomenclature (JCBN) (1984) *Eur. J. Biochem. 138*, 9–37.

Jardetzky, O., & Roberts, G. C. K. (1981) *NMR in Molecular Biology*, Academic Press. New York.

Kessler, H., Bermel, W., Müller, A., & Pook, K.-H. (1985) in *The Peptides—Analysis, Synthesis, Biology. Volume 7: Conformation in Biology and Drug Design* (Hruby, V. J., Ed.) pp 437–473, Academic Press, Orlando, Florida.

Kojro, E., Gwizdala, E., & Grzonka, Z. (1987) *Pol. J. Chem. 61*, 415–424.

Kopple, K. D., Ohnishi, M., & Go, A. (1969a) *J. Am. Chem. Soc. 91*, 4264–4272.

Kopple, K. D., Ohnishi, M., & Go, A. (1969b) *Biochemistry 8*, 4087–4095.

Kumar, N. G., & Urry, D. W. (1973) *Biochemistry 12*, 4392–4399.

Lancaster, R. (1990) M.Sc. Thesis, McMaster University, Hamilton, Ontario, Canada.

Lemaire, S., Chouinard, L., Denis, D., Panico, M., & Morris, H. R. (1982) *Biochem. Biophys. Res. Commun. 108*, 51–58.

Lemaire, S., Valette, A., Chouinard, L., Dupuis, N., Day, R., Porthe, G., & Cros, J. (1983) *Neuropeptides 3*, 181–191.

Llinás, M., & Klein, M. P. (1975) *J. Am. Chem. Soc. 97*, 4731–4737.

Marion, D., & Wüthrich, K. (1983) *Biochem. Biophys. Res. Commun. 113*, 967–974.

Maroun, R., & Mattice, W. L. (1981) *Biochem. Biophys. Res. Commun. 103*, 442–446.

Mattice, W. L., & Robinson, R. M. (1981) *Biophys. Res. Commun. 101*, 1311–1317.

McDonald, C. C., & Phillips, W. D. (1967) *J. Am. Chem. Soc. 89*, 6332–6341.

Millan, M. J. (1990) *Trends Pharmacol. Sci. 11*, 70–76.

Morley, J. S. (1983) *Br. Med. Bull. 39*, 5–10.

Nakajima, K., Erne, D., Bean, J. W., Sargent, D. F., Schwyzer, R., Paterson, S. J., & Kosterlitz, H. W. (1988) *Tetrahedron 44*, 721–732.

Neuhaus, D., & Williamson, M. P. (1989) *The Nuclear Overhauser Effect in Structural and Conformational Analysis*, VCH Publishers, New York.

Ohnishi, M., & Urry, D. W. (1969) *Biochem. Biophys. Res. Commun. 36*, 194–202.

Pachler, K. G. R. (1964) *Spectrochim. Acta 20*, 581–587.

Pardi, A., Billeter, M., & Wüthrich, K. (1984) *J. Mol. Biol. 180*, 741–751.

Piantini, U., Sørensen, O. W., & Ernst, R. R. (1982) *J. Am. Chem. Soc. 104*, 6800–6801.

Pitner, T. P., & Urry, D. W. (1972) *J. Am. Chem. Soc. 94*, 1399–1400.

Pople, J. A., Schneider, W. G., & Bernstein, H. J. (1959) *High Resolution NMR*, McGraw-Hill, New York.

Rance, M., Sørensen, O. W., Bodenhausen, G., Wagner, G., Ernst, R. R., & Wüthrich, K. (1983) *Biochem. Biophys. Res. Commun. 117*, 479–485.

Rapaka, R. S., Renugopalakrishnan, V., Collette, T. W., Dobbs, J. C., Carreira, L. A., & Bhatnagar, R. S. (1987a) *Int. J. Pept. Protein Res. 30*, 284-287.
Rapaka, R. S., Renugopalakrishnan, V., Huang, S.-G., Dobbs, J. C., & Carreira, A. (1987b) in *Tenth American Peptide Symposium Abstracts*, P-205, Washington University, St. Louis, MO.
Renugopalakrishnan, V., Rapaka, R. S., Huang, S.-G., Moore, S., & Hutson, T. B. (1988) *Biochem. Biophys. Res. Commun. 151*, 1220-1225.
Sargent, D. F., & Schwyzer, R. (1986) *Proc. Natl. Acad. Sci. U.S.A. 83*, 5774-5778.
Schiller, P. W. (1983) *Int. J. Pept. Protein Res. 21*, 307-312.
Schwyzer, R. (1986) *Biochemistry 25*, 4281-4286.
Schwyzer, R., & Ludescher, U. (1969) *Helv. Chim. Acta 52*, 2033-2040.
Sober, H. A., Ed. (1970) *CRC Handbook of Biochemistry, Selected data for molecular biology*, 2nd ed., The Chemical Rubber Co., Cleveland, OH.
States, D. J., Haberkorn, R. A., & Ruben, D. J. (1982) *J. Magn. Reson. 48*, 286-292.
Surewicz, W. K., & Mantsch, H. H. (1988) *Biochim. Biophys. Acta 952*, 115-130.
Surewicz, W. K., & Mantsch, H. H. (1989) *J. Mol. Struct. 214*, 143-147.
Tachabina, S., Araki, K., Ohya, S., & Yoshida, S. (1982) *Nature (London) 295*, 339-340.
Tappin, M. J., Pastore, A., Norton, R. S., Freer, J. H., & Campbell, I. D. (1988) *Biochemistry 27*, 1643-1647.
Taylor, J. W. (1990) *Biochemistry 29*, 5346-5373.
Taylor, J. W., & Kaiser, E. T. (1986) *Pharmacol. Rev. 38*, 291-319.
Turcotte, A., Lalonde, J. M., St.-Pierre, S., & Lemaire, S. (1984) *Int. J. Pept. Protein Res. 23*, 361-367.
Urry, D. W., Masotti, L., & Krivacic, J. R. (1971) *Biochim. Biophys. Acta 241*, 600-612.
Wu, C.-S. C., & Yang, J. T. (1981) *Mol. Cell. Biochem. 40*, 109-122.
Wüthrich, K. (1986) *NMR of Proteins and Nucleic Acids*, Wiley-Interscience, New York.
Yang, J. T., Bewley, T. A., Chen, G. C., & Li, C. H. (1977) *Proc. Natl. Acad. Sci. U.S.A. 74*, 3235-3238.
Yang, J. T., Wu, C.-S. C., & Martinez, H. M. (1986) *Methods Enzymol. 130*, 208-269.
Zhou, N., & Gibbons, W. A. (1986) *J. Chem. Soc., Perkin Trans. 2*, 637-644.

Fluoroaluminum and Fluoroberyllium Nucleoside Diphosphate Complexes as Probes of the Enzymatic Mechanism of the Mitochondrial F_1-ATPase†

Jean Paul Issartel,* Alain Dupuis, Joël Lunardi, and Pierre V. Vignais
Laboratoire de Biochimie, Département de Biologie Moléculaire et Structurale, Centre d'Etudes Nucléaires de Grenoble, 85X, 38041 Grenoble Cedex, France

Received March 26, 1990; Revised Manuscript Received February 5, 1991

ABSTRACT: The mechanism by which fluoride and aluminum or beryllium in combination with ADP inhibit beef heart mitochondrial F_1-ATPase was investigated. The kinetics of inhibition depended on the nature of the anion present in the F_1-ATPase assay medium. Inhibition required the presence of Mg^{2+} and developed more rapidly with sulfite and sulfate than with chloride, i.e., with anions which activate F_1-ATPase activity. The ADP-fluorometal complexes were bound quasi-irreversibly to F_1, and each mole of the inhibitory nucleotide-fluorometal complex was tightly associated with 1 mol of Mg^{2+}. One mole of nucleotide-fluorometal complex was able to inhibit the activity of 1 mol of catalytic site in F_1. Direct measurements of bound fluoride, aluminum, beryllium, and ADP indicated that the F_1-bound ADP-fluorometal complexes are of the following types: $ADP_1Al_1F_4$, $ADP_1Be_1F_1$, $ADP_1Be_1F_2$, or $ADP_1Be_1F_3$. Fluoroaluminates or fluoroberyllates are isomorphous to P_i, and the inhibitory nucleotide-fluorometal complexes mimicked transient intermediates of nucleotides that appeared in the course of ATP hydrolysis. On the other hand, each mole of fully inhibited F_1 retained 2 mol of inhibitory complexes. The same stoichiometry was observed when ADP was replaced by GDP, a nucleotide which, unlike ADP, binds only to the catalytic sites of F_1. These results are discussed in terms of a stochastic model in which the three cooperative catalytic sites of F_1 function in interactive pairs.

In the presence of magnesium ions, three out of six nucleotide binding sites that are present in mitochondrial F_1-ATPase[1] exchange their bound ADP or ATP with medium nucleotides, whereas the other three retain their bound nucleotides in a tightly associated form (Cross et al., 1982: Kironde & Cross, 1986). The three exchangeable binding sites are thought to be catalytic and to act in a cooperative manner (Gresser et al., 1982: Cross et al., 1982). Besides the catalytic sites, regulatory sites have been proposed to account for the unusual kinetic behavior of F_1 under specific conditions (Di Pietro et al., 1980; Wang, 1984; Weber et al., 1985). We recently reported that F_1-ATPase is inhibited by aluminum or beryllium in the presence of fluoride and ADP (Lunardi et al., 1988). A possible explanation was that fluoroaluminum and fluoro-

† This work was supported by grants from the Centre National de la Recherche Scientifique (URA/CNRS 1130), the Faculté de Médecine, Université Joseph Fourier de Grenoble, and the "Association Française contre les Myopathies".

[1] Abbreviations: F_1-ATPase, catalytic sector (soluble) of the beef heart mitochondrial ATPase complex; p*F*, colog of the free fluoride concentration; AMPPNP, 5'-adenylyl imidodiphosphate.

0006-2960/91/0430-4726$02.50/0